

Natural genetic variation in wild-derived mice controls host survival and transcriptional responses during endotoxic shock

Bristy Sabikunnahar ¹, Julia P. Snyder¹, Princess D. Rodriguez², Katherine J. Sessions¹, Eyal Amiel ¹, Seth E. Fietze¹, and Dimitry N. Krementsov ^{1,*}

¹Department of Biomedical and Health Sciences, University of Vermont, Burlington, VT, United States

²Department of Microbiology and Molecular Genetics, University of Vermont, Burlington, VT, United States

*Corresponding author: Department of Biomedical and Health Sciences, University of Vermont, 312C Rowell bldg, 106 Carrigan drive, Burlington, VT, United States. Email: dkrement@uvm.edu.

Abstract

Innate immune cells sense microbial danger signals, resulting in dynamic transcriptional reprogramming and rapid inflammatory responses. If not properly regulated, such responses can be detrimental to the host, as is seen in septic shock. A better understanding of the genetic regulation of responses during endotoxemia could provide potential therapeutic insights. However, the majority of animal model studies have been performed using classic inbred laboratory strains of mice, capturing limited genetic diversity. Here, we compared classic inbred C57BL/6 (B6) mice with wild-derived and genetically divergent PWD/PhJ (PWD) mice using in vivo and in vitro models of endotoxemia. Compared with B6 mice, PWD mice were markedly resistant to bacterial lipopolysaccharide (LPS)-induced endotoxic shock. Using LPS stimulation of bone marrow derived dendritic cells (BMDC) and RNA sequencing, we demonstrate that B6 and PWD BMDCs exhibit partially overlapping yet highly divergent transcriptional responses, with B6 skewed toward stereotypical proinflammatory pathway activation, and PWD engaging regulatory or developmental pathways. To dissect genetic regulation of inflammatory responses by allelic variants, we used BMDCs from a sub-consomic strain carrying a ~50 Mb PWD-derived portion of chromosome 11 on the B6 background. This identified a subset of cis-regulated and a large number of trans-regulated genes. Bioinformatic analyses identified candidate trans regulators encoded in the chromosome 11 locus as transcription factors *Irf1*, *Ncor1*, and *Srebf1*. Our results demonstrate that natural genetic variation controls host survival and transcriptional reprogramming during endotoxemia, suggesting possibilities for prediction of sepsis risk and/or personalized therapeutic interventions.

Keywords: animals-rodent, cells-dendritic cells, diseases-endotoxic shock, molecules-lipopolysaccharide, processes-gene regulation

Introduction

Sepsis is a life-threatening medical condition that causes thousands of deaths and costs billions of dollars in healthcare annually in the United States alone.¹ Septic shock occurs when the body's dysregulated inflammatory response to poorly contained systemic infection leads to tissue damage, organ dysfunction, and even death.²

Innate immune cell activation is the first critical factor in septic shock induction, and it occurs as different pattern recognition receptors (PRRs) on macrophages and other myeloid cells recognize pathogen-associated molecular patterns (PAMPs) such as bacterial lipopolysaccharide (LPS).^{3,4} Since 1930, when LPS was recognized as a critical endotoxin driving human sepsis, murine LPS-induced endotoxemia models have become an accessible and reproducible research tool utilized to study the molecular physiology of acute inflammatory responses driving septic shock, although it has limited utility as a true preclinical model of sepsis.⁵ PRR activation causes dynamic transcriptional reprogramming and rapid inflammatory responses, including systemic production of pro-inflammatory cytokines and chemokines.^{6,7} PRRs can also recognize damage-associated molecular patterns (DAMPs) released from damaged tissue, leading to excessive activation of immune cells and endothelial cells.⁸ These phenomena cause the overproduction of cytokines such as tumor necrosis factor

α (TNF- α) and interleukin (IL)-6, which in turn can result in loss of vascular endothelial integrity, drop in blood pressure, systemic coagulation, and other pathologic sequelae that can ultimately result in death.³

Despite its importance as a public health problem, development of effective therapeutic agents for treating sepsis has been challenging. Many therapeutic agents have entered the clinical trials but universally failed to demonstrate efficacy in humans, in spite of showing tremendous promise in preclinical animal models.^{9–11} Notably, these preclinical studies have historically been almost exclusively done using classic inbred laboratory strains of mice, typically C57BL/6 (B6), thus capturing limited genetic diversity. Hence, to bridge the gap between immense genetic diversity of human populations and current preclinical studies, in this present study, we utilized a so-called wild-derived strain of mice, PWD/PhJ (PWD).¹² We and others have shown previously that the disease phenotypes and immune cell transcriptional responses between classic laboratory strains and wild-derived strains of mice, including PWD, are divergent during homeostasis and in different models of immune-mediated pathology.^{13–19} Other studies, using mouse models of sepsis, have previously documented phenotypic differences between classic lab strains like B6 and other wild-derived strains, namely, MOLF/Ei and SPRET/Ei, with a number of candidate genes driving

Received: September 12, 2024. Accepted: January 22, 2025

© The Author(s) 2025. Published by Oxford University Press on behalf of The American Association of Immunologists.

This is an Open Access article distributed under the terms of the Creative Commons Attribution-NonCommercial License (<https://creativecommons.org/licenses/by-nc/4.0/>), which permits non-commercial re-use, distribution, and reproduction in any medium, provided the original work is properly cited. For commercial re-use, please contact reprints@oup.com for reprints and translation rights for reprints. All other permissions can be obtained through our RightsLink service via the Permissions link on the article page on our site—for further information please contact journals.permissions@oup.com.

differential responses *in vivo* and *in vitro* successfully mapped and identified.^{20,21} However, the susceptibility of the unique PWD strain, or the closely related PWK/PhJ strain¹² to septic shock remains unknown.

In this study, we assessed the role of natural genetic variation in septic shock clinical outcomes and transcriptional reprogramming using *in vivo* and *in vitro* acute LPS endotoxemia model in classic B6 and wild-derived PWD mice. We used bone marrow derived-dendritic cells (BMDCs) as an *in vitro* innate immune cell model to examine transcriptional regulation upon LPS stimulation via RNA-seq. Furthermore, to dissect the genetic regulation of inflammatory responses by allelic variants, we employed BMDCs from a sub-consomic strain that carries approximately 50 Mb of PWD-derived chromosome 11 (Chr11) on a B6 background. Our study demonstrates that PWD mice, compared to B6 mice, exhibit greater resistance to sickness and mortality during LPS endotoxemia and display divergent transcriptional responses in LPS-stimulated BMDCs. Additionally, we found that PWD-derived allelic variants on Chr11 robustly regulate gene expression in *cis* and *in trans*, the latter likely via differential transcription factor activity. Altogether, this study suggests that natural genetic variation impacts sickness behavior and host survival during LPS endotoxemia in conjunction with profound differences in transcriptional regulation in myeloid cells.

Materials and methods

Animals

Three mouse strains were used in this study, C57BL/6J (Jackson Laboratory Stock #000664; B6), C57BL/6J-Chr 11.2^{PWD/PhJ}/ForeJ (Jackson Laboratory Stock cat. no. 005998; 11.2), and PWD/PhJ (Jackson Laboratory Stock cat. no. 004660; PWD). All mice were originally purchased from Jackson laboratories and bred at the vivarium at the University of Vermont for 5 to 7 generations prior to generating experimental animals. Mice were housed in individually ventilated cages with HEPA-filtered air (2 to 5 of 1 sex/strain per cage) and fed standard rodent chow pellets (Purina, USA). The coordinates of the PWD-derived interval on chromosome 11 in 11.2 congenic mice were determined using genotyping at the DartMouse Core Facility (Dartmouth College, New Hampshire, USA) as previously described.^{15,22,23} Adult mice (8 to 12 weeks of age) were used for all experiments, including mice used for the generation of primary BMDC cultures and mice used for LPS challenge experiments. All the experimental procedures were approved by the Institutional Animal Care and Use Committee of the University of Vermont.

In vivo LPS challenge experiments

Age- and sex-matched male and female mice in each strain were injected intraperitoneally (i.p.) with *E. coli* LPS O26: B6 (Sigma Aldrich, St Louis, Missouri, USA) at 50 mg/kg body weight (lower dose) and at 70 mg/kg (higher dose). LPS-challenged mice were monitored for survival and semi-quantitative evaluation of clinical signs induced by the sickness responses for 96 h. A clinical scoring system was adapted from previous study²⁴ with minor modifications, as follows, 0 = no abnormal clinical signs, 1 = ruffled fur but lively, 2 = ruffled fur, moving slowly, hunched, and sick, 3 = ruffled fur, squeezed eyes, hardly moving, down, and very sick, 4 = same as 3 but with incontinence, 5 = moribund or dead.

For serum cytokine analysis, mice were injected with a different, more potent batch of *E. coli* LPS O26: B6 (Sigma Aldrich, St Louis, Missouri, USA) at 20 mg/kg, body weight and blood was collected at different time points and analyzed. Blood was incubated for 30 min at room temperature to allow clotting, followed by storage on ice for 1 to 2 h, centrifugation, and collection of serum.

Cell culture

Male and female B6, 11.2, and PWD mice were humanely euthanized by CO₂ asphyxiation, followed by extraction of femurs and tibias, and isolation of bone marrow cells by flushing with the bones with PBS. Primary bone marrow-derived dendritic cells (BMDCs) were generated from mouse bone marrow cells using a standard 7-day granulocyte-macrophage colony-stimulating factor (GM-CSF, 20 ng/ml, Shenandoah cat. no. 200-15) differentiation protocol, as previously described.¹⁵ Each mouse was used to generate an independent BMDC culture that was treated as a single biological replicate (the number of biological replicates for different experiments is indicated in each figure legend). BMDCs were cultured in complete medium (RPMI 1640 containing 10% FBS, 2 mM L-glutamine, 100 Units/ml penicillin, 100 µg/ml streptomycin, and 55 µM beta-mercaptoethanol, all from Gibco). BMDCs were seeded in 1 million per well and were either unstimulated (control) or stimulated with the TLR-4 ligand lipopolysaccharide (LPS) from *E. coli* 0111: B4 (InvivoGen, San Diego, California, USA) at 10 ng/ml, followed by RNA isolation for RNAseq, or cytokine assays on the cell supernatants, as described below. Separate BMDC cultures were generated for RNAseq experiments and for cytokine assays, with the number of biological replicates indicated in the figure legends. For RNAseq, cells were collected for RNA extraction after 6 h of stimulation with LPS (as well as from the unstimulated controls in parallel). For cytokine assays, cell culture supernatants were collected at 24 h post-stimulation with LPS.

Cytokine quantification by ELISA

For the detection of cytokines in the cell culture supernatants or sera, we performed ELISAs as described previously,²⁵ using the primary capture mAbs anti-TNF-α, and anti-IL-6, and their corresponding biotinylated detection mAbs (BioLegend, San Diego, California, USA). Other ELISA reagents included recombinant mouse TNF-α, and IL-6 as standards (BioLegend, San Diego, California, USA), HRP-conjugated avidin D (Vector Laboratories, Burlingame, California, USA), and tetramethylbenzidine microwell peroxidase substrate and stop solution (Kirkegaard and Perry Laboratories, Gaithersburg, Maryland, USA). Biological replicates were used, representing independent BMDC cultures from individual mice (cell culture) or sera from individual mice (in vivo experiments).

RNAseq and bioinformatic analysis

Four biological replicates per genotype (2 of each sex per genotype), each replicate representing an independent BMDC culture from an individual mouse, were used. BMDCs were seeded at 1 × 10⁶ cells/well in a 12 well plate and treated with LPS at 10 ng/ml concentration for 6 h. RNA was extracted according to the manufacturer's instructions using the RNeasy plus Mini Kit (cat no. 74104) by Qiagen (Hilden, Germany), followed by quantification by Qubit and quality

assessment by BioAnalyzer. A starting input of 1 μ g of total RNA was used for ribosomal RNA depletion with the NEBNext rRNA Depletion kit. Stranded cDNA libraries were then prepared with the NEBNext Ultra II Directional RNA Library Prep Kit (New England Biolabs, Ipswich, Massachusetts, USA) according to the manufacturer's protocol. Paired end 150 bp sequencing was performed on an Illumina HiSeq1500.

Demultiplexed sequencing data was received from the sequencing facilities and quality control of the sequencing data was done using FastQC platform. Genomic alignment of the RNA-seq data was performed using STAR (v2.7.11b) tool²⁶ using the mouse genome assembly GRCm39 (mm39). Number of reads per gene was quantified by quantMode GeneCounts. Raw sequencing data and normalized per gene count matrix were deposited in GEO (accession no. GSE272206). Differential gene-expression analyses were conducted using DESeq2.²⁷ Cutoffs for differential gene expression are described in the Results section. Gene-specific P values for differential expression were adjusted for multiple comparisons using the Benjamini-Hochberg method as implemented in DESeq2.²⁷ Gene ontology (GO) enrichment analysis of differentially expressed genes was performed using PANTHER.²⁸ The decoupleR tool²⁹ was used to analyze differentially expressed gene sets to quantify enrichment of predicted transcription factor activity, based on known gene targets. decoupleR was also used to identify putative specific transcription factor-regulated gene targets within differentially expressed gene sets.

The Mouse Phenome Database SNP query tool was used to determine the non-synonymous single nucleotide polymorphisms (nsSNPs) between B6 and PWD mice. We used PWK/PhJ as a proxy for PWD, because of the availability of deep genotyping data on the former. Functional domains of transcription factors in Fig. 6 were made by integrating domain information from relevant articles,^{30–33} UniProt, and NCBI (Fig. 6J, K).

Statistical analyses

In the manuscript, “n” refers to individual mice (or individual BMDC cultures from individual mice) and the numbers of mice used in each experiment is described in the figure legends. Statistical analyses (other than RNAseq; see above) were carried out using GraphPad Prism software version 10.2.1 (GraphPad Software, San Diego, California, USA). The specific tests used to assess the significance of the observed differences are detailed in the figure legends. All center values represent the mean, and error bars represent the standard error of the mean (SEM). A P-value of <0.05 was considered significant.

Results

PWD mice are resistant to LPS-induced endotoxemia

To investigate the effect of natural genetic variation on the inflammatory response during septic shock, we employed the LPS endotoxemia model by administering LPS (*E. coli* O26: B6) intraperitoneally (i.p.) to classic laboratory B6 mice and wild-derived PWD mice. Initially, we challenged the mice with a sublethal dose (50 mg/kg body weight) of LPS (Fig. 1A–C), followed by monitoring of weight loss and quantitative evaluation of clinical signs induced by the sickness responses, as previously described,^{24,25,34} at individual time

points, and as a cumulative variable, using area under the curve (AUC) analysis. We found that upon LPS challenge, PWD mice lost weight faster than B6 mice; however, they also began to recover weight loss more readily compared to B6 (Fig. 1A). Importantly, we found that PWD mice showed significantly reduced clinical signs compared with B6 mice, followed by complete recovery by 36 h post-challenge (Fig. 1B, C). These data suggest that PWD mice are more resistant to sickness responses induced by systemic endotoxin challenge than B6 mice.

Next, we have challenged the mice with a high dose (70 mg/kg) of LPS to study survival, in addition to weight loss and quantitative evaluation of clinical signs (Fig. 1D–K). Like the lower dose, we found that while PWD mice lost more weight initially than the B6 mice, they began to recover more quickly (Fig. 1D). Additionally, PWD mice exhibited significantly reduced sickness responses and mortality, with complete recovery by 96 hours in 100% of the mice, while B6 mice exhibited progressively worsening clinical signs, with 85% of the mice succumbing to the challenge (Fig. 1E–G). Previous studies in humans and animal models have suggested that sex is an important biological variable in sepsis outcomes.³⁵ We therefore reanalyzed these data segregated by sex. There was no significant difference in weight loss between males and females within each genotype (Fig. 1H). However, we found that females of both genotypes were significantly more susceptible to acute sickness during LPS endotoxemia than males (Fig. 1I, J). Similarly, B6 females exhibited significantly increased mortality (100%) compared with B6 males (67%), although PWD mice had 0% mortality regardless of sex (Fig. 1K). Taken together, these results demonstrate that, compared with B6 mice, PWD mice are significantly more resistant to LPS endotoxemia-related sickness behavior and mortality. They also suggest that female mice are more susceptible to LPS-induced endotoxemia than male mice independent of genotype.

Myeloid cells derived from B6 and PWD mice exhibit conserved and highly divergent gene expression patterns upon LPS stimulation

TLR activation of myeloid cells *in vitro* represents a tractable model to understand molecular mechanisms underlying inflammatory responses in sepsis. To investigate the effects of natural genetic variation on transcriptional regulation of myeloid cell inflammatory responses that could lead to divergent endotoxemia responses and survival *in vivo*, we conducted bulk RNA-seq analysis on bone marrow-derived dendritic cells (BMDCs) isolated from B6 and PWD mice. BMDCs were either left untreated or stimulated with LPS (10 ng/ml) for 6 h, followed by RNA isolation and RNA-seq analysis. Principal component analysis demonstrated distinct sample clustering by treatment and genotype, with genotype surprisingly accounting for a much greater proportion of variance (Fig. 2A). First, to assess the inflammatory transcriptional response in each genotype, we performed differential gene expression analyses comparing LPS vs untreated conditions within each genotype (Fig. 2B–F). This analysis revealed that thousands of genes were differentially expressed upon LPS stimulation in both B6 and PWD BMDCs (Fig. 2B, C). The total number of differentially expressed genes (DEGs) was greater in B6 BMDCs (3,349 genes) compared to PWD BMDCs (2,334 genes), with an overlap of 1,411 genes between both groups, while the rest were unique to each

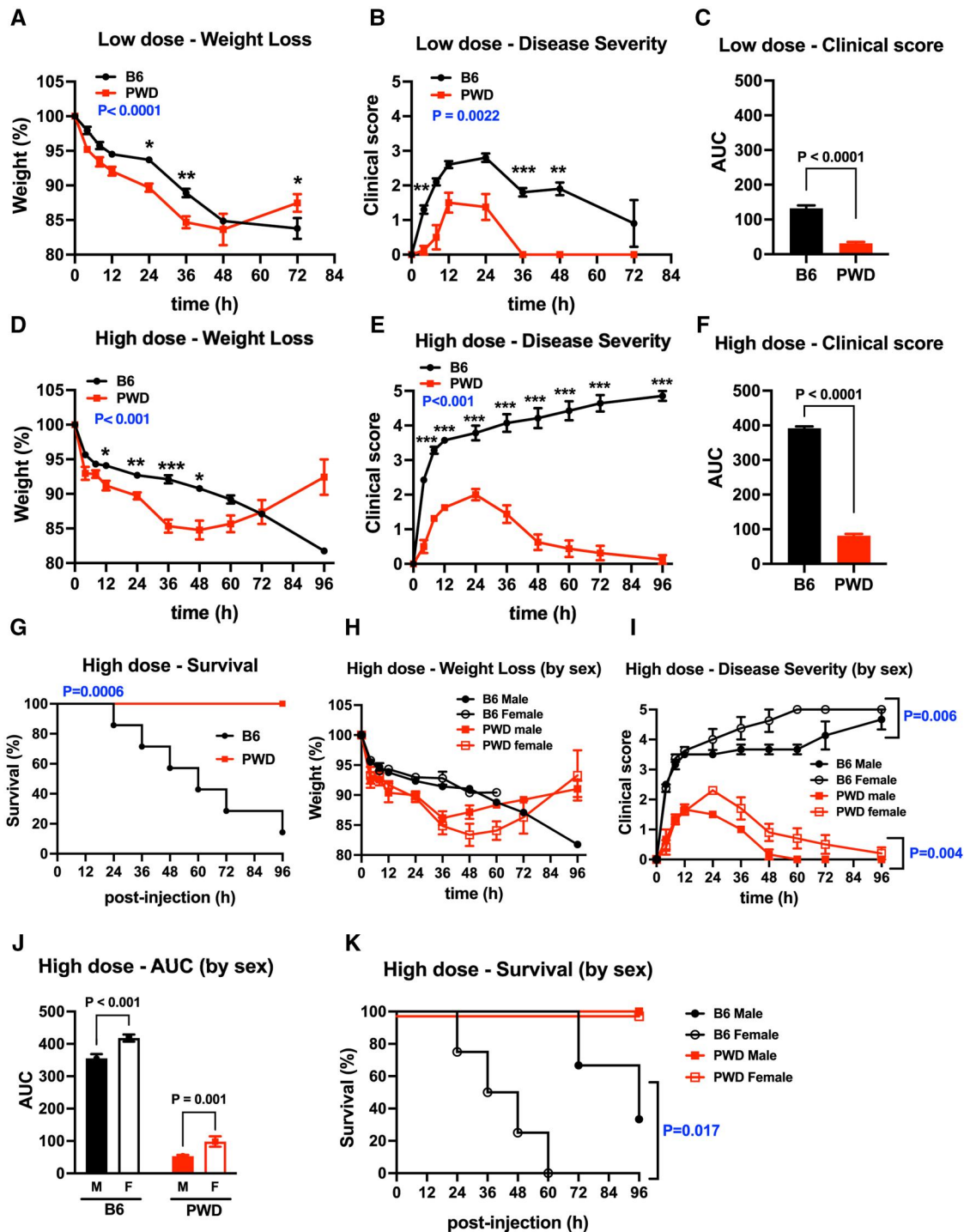


Figure 1. PWD mice are more resistant to LPS-induced endotoxemia compared with B6 mice. (A–C) B6 (n = 5) and PWD (n = 4) all female mice were challenged with 50 mg/kg (denoted as Low dose) LPS i.p., followed by evaluation of weight loss (A) and sickness behavior (B) at different time points. Area under the curve (AUC) analysis (C) was calculated from kinetic data in panel B, to calculate a cumulative measurement of the disease severity. Clinical score evaluation is described in the Methods section. (D–K) Male and female B6 (n = 7, 3M, 4F) and PWD (n = 8, 3M, 5F) mice were injected with 70 mg/kg (denoted as High dose) LPS i.p., followed by monitoring weight loss (D) and clinical signs (E) at different time points up to 96 hrs. (F) AUC was analyzed from the kinetic data from panel E, to show a cumulative measurement of disease severity. (G) Survival analysis was performed on the high dose LPS challenged mice. (H–J) Data from the high dose LPS challenge experiment depicted in D–G, segregated by sex for both the genotypes, with weight loss, clinical score and AUC analysis are shown in panels H, I and J, respectively. (K) Survival in B6 and PWD mice is shown in panel G for all the mice, then sex-separated survival analysis for each genotype is shown in Panel K. Significance of differences was assessed using 2-way ANOVA or mixed model for panel A, B, D, E, H, I, and J (with Sidák test for post-hoc pairwise comparisons), Welch's T test for panel C and F, Mantel-Cox test for panel G and K. Here, P value in blue color describes time x genotype interaction in panels A, B, D, and E and time x sex interaction in panel I. P values are represented as follows: * = ≤ 0.033 , ** = ≤ 0.002 , *** = ≤ 0.001 or otherwise mentioned in the figure.

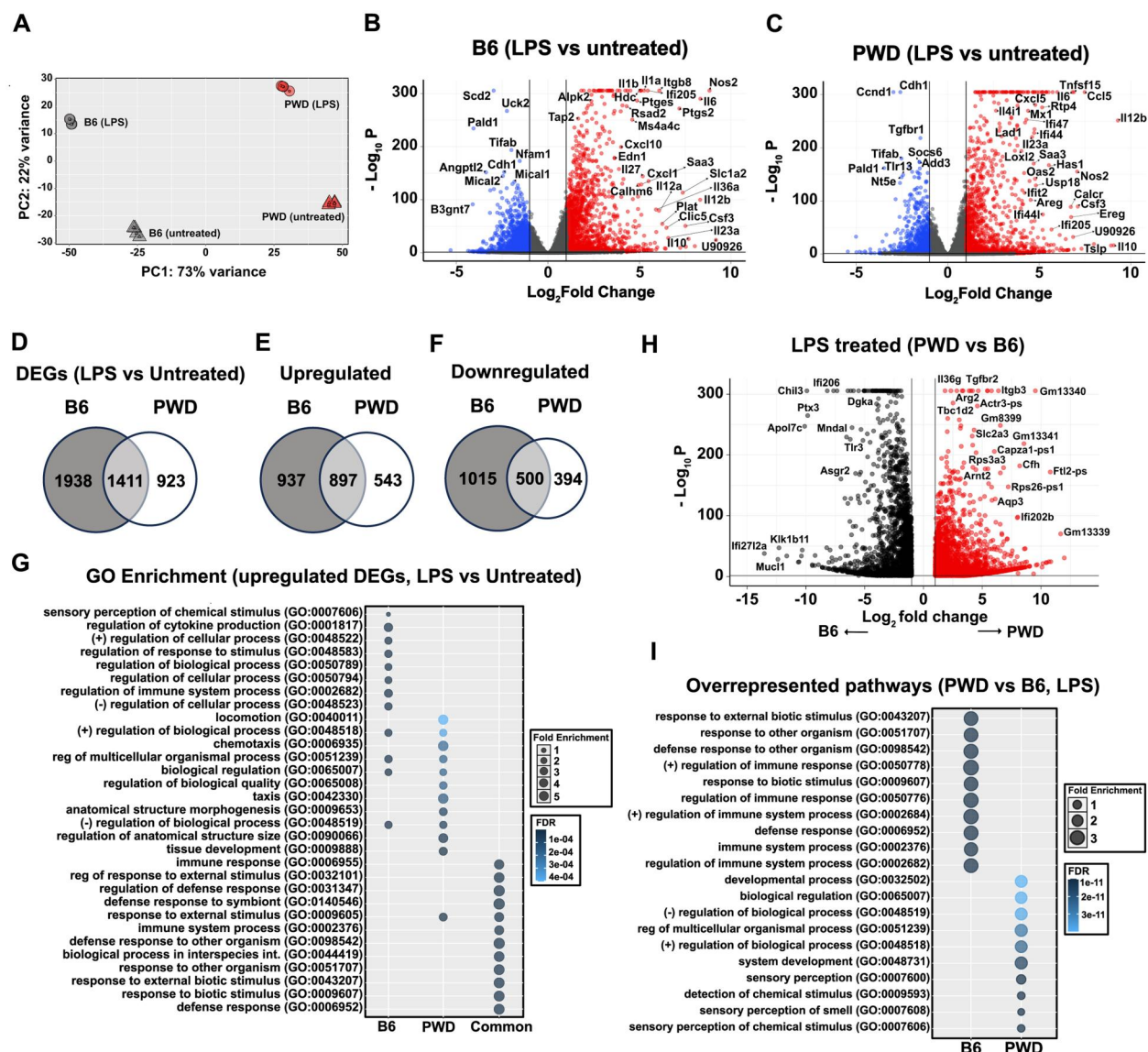


Figure 2. B6 and PWD myeloid cells show differential transcriptional regulation upon LPS treatment. BMDC cultures were generated from B6 ($n = 4$, 2 of each sex) and PWD ($n = 4$, 2 of each sex) mice, treated with LPS (10 ng/ml) for 6 h or left untreated, followed by RNA extraction and RNA-seq analysis using the DESeq2 package. Differentially expressed genes (DEGs) for all contrasts were determined using a cutoff of $\text{Padj} < 0.05$ and $|\text{Log}_2\text{Fold}| \geq 1$. (A) Principal component analysis, demonstrating clustering of individual samples by genotype and treatment, as annotated. (B, C) Volcano plots showing the DEGs from LPS vs untreated contrast in B6 and PWD BMDC, respectively. Highly significant genes were annotated by enhanced volcano tool that passed the cutoff. (D–F) Venn diagrams comparing LPS-dependent DEGs in B6 and PWD BMDCs, shown as total DEGs, or subsetted into upregulated and downregulated DEGs, as indicated. (G) LPS-upregulated DEGs unique to B6, PWD, or common to both were subjected to GO pathway enrichment analysis using PANTHER. Top 12 pathways for each group based on FDR are shown. (H) Volcano plot showing DEGs overrepresented in B6 or PWD LPS-activated BMDCs (PWD LPS vs B6 LPS contrast). Highly significant genes were annotated by enhanced volcano tool. (I) DEGs overrepresented in B6 or PWD LPS-activated BMDCs were subjected to GO pathway enrichment analysis using PANTHER. Top 10 pathways based on FDR for each genotype are shown in the figure.

genotype (Fig. 2D), indicating the presence of both conserved stereotypical responses to LPS and unique divergent responses in PWD compared with B6. We found a similar pattern when upregulated and downregulated genes were analyzed separately (Fig. 2E, F). According to our interest in the difference between B6 and PWD immune activation, we focused on the upregulated DEGs, to identify molecular pathways associated with these distinct genotype-dependent transcriptional profiles. We performed enrichment analysis using Gene Ontology (GO) on sets of upregulated DEGs (LPS vs untreated) that were either unique to B6 and PWD, or shared between both the genotypes (Fig. 2G). As expected, common upregulated DEGs in both strains were linked to

many major immune response pathways, including *defense response*, *response to organisms*, and *regulation of immune response to external stimulus* (Fig. 2G). We found that the biological processes that were associated with unique DEGs upregulated in B6 notably included *cellular process regulation*, *stimulus response regulation*, and *cytokine production regulation*. Interestingly, PWD-unique upregulated DEGs were associated significantly with pathways important for development: eg *tissue development* and *regulation of anatomical structure*, as well as cell motility: for example, *taxis* and *locomotion*. Taken together, these data demonstrate that both B6 and PWD myeloid cells exhibit robust yet distinct transcriptional response upon LPS stimulation.

As a parallel approach to more directly assess gene expression differences between PWD and B6 myeloid cells after activation, we performed differential gene expression analysis by comparing B6 to PWD BMDCs after LPS stimulation. In this comparison, we found that distinct gene sets are overrepresented in each genotype (Fig. 2H). GO enrichment analyses on the overrepresented gene sets in LPS treated B6 and PWD BMDCs revealed distinct biological process involvement for each (Fig. 2I). Overrepresented genes in B6 BMDCs exhibited association with important immune pathways like *defense response*, *positive regulation of immune system process*, and *response to external biotic stimulus*, involving key immune response genes such as *Nos2*, *C3*, *Stat5*, *Tlr3*, *Ccl7*, *Ido1*, *Ifi208*, *Vcam1*, *Ccl12*, *Il6*, and *Cxcl10* (Fig. 2I and File S1). Conversely, overrepresented gene sets in PWD strain showed links with pathways related to developmental processes, for example, *regulation of multicellular organismal process*, *biological regulation*, and *detection of chemical stimulus*, involving genes like *Olfr482*, *Cald1*, *Bmp4*, *Cxcl5*, *Bcl6b*, *Cep290*, *Zfp566*, *Slc2a3*, *Arg2*, and *Itgb3* (Fig. 2I and File S1). Interestingly, a significant number of PWD-enriched genes were unannotated transcripts/putative pseudogenes, such as *Gm13339*, *Ftl2-ps*, and *Actr3-ps*, suggesting that these may in fact represent functional genes of interest in PWD (Fig. 2H and File S1). Collectively, these data suggest that natural genetic variation drives differential transcriptional responses

during inflammatory activation of myeloid cells, with the PWD genotype diverging from the stereotypical proinflammatory response seen in B6, which has been the focus of the majority of previous mouse model studies.

LPS-induced pro-inflammatory cytokine production and release are decreased in PWD mice compared to B6 mice

TLR-4 activation causes acute inflammatory responses by triggering the release of a number of pro-inflammatory cytokines that are a hallmark of LPS-induced septic shock.³⁶ We therefore assessed how natural genetic variation in mice can affect synthesis and secretion of two key LPS-induced pro-inflammatory cytokines: TNF- α and IL-6, which are known to regulate survival during LPS endotoxemia.^{37–39} First, we examined mRNA expression of *Tnfa* and *Il6* in B6 and PWD BMDCs in our RNA-seq data. We found that while *Il6* was among the genes significantly overrepresented in LPS-stimulated B6 BMDCs compared with PWD, whereas *Tnfa* did not pass the cutoff for PWD vs B6 differential expression (File S1). In a standalone post hoc analysis, we found that *Tnfa* and *Il6* mRNAs, while robustly induced by LPS stimulation in both genotypes, were expressed at significantly lower levels in PWD mice compared to B6 mice after LPS treatment (Fig. 3A, B). This was validated at the protein level by ELISA, with significantly less TNF- α and IL-6 secreted by PWD

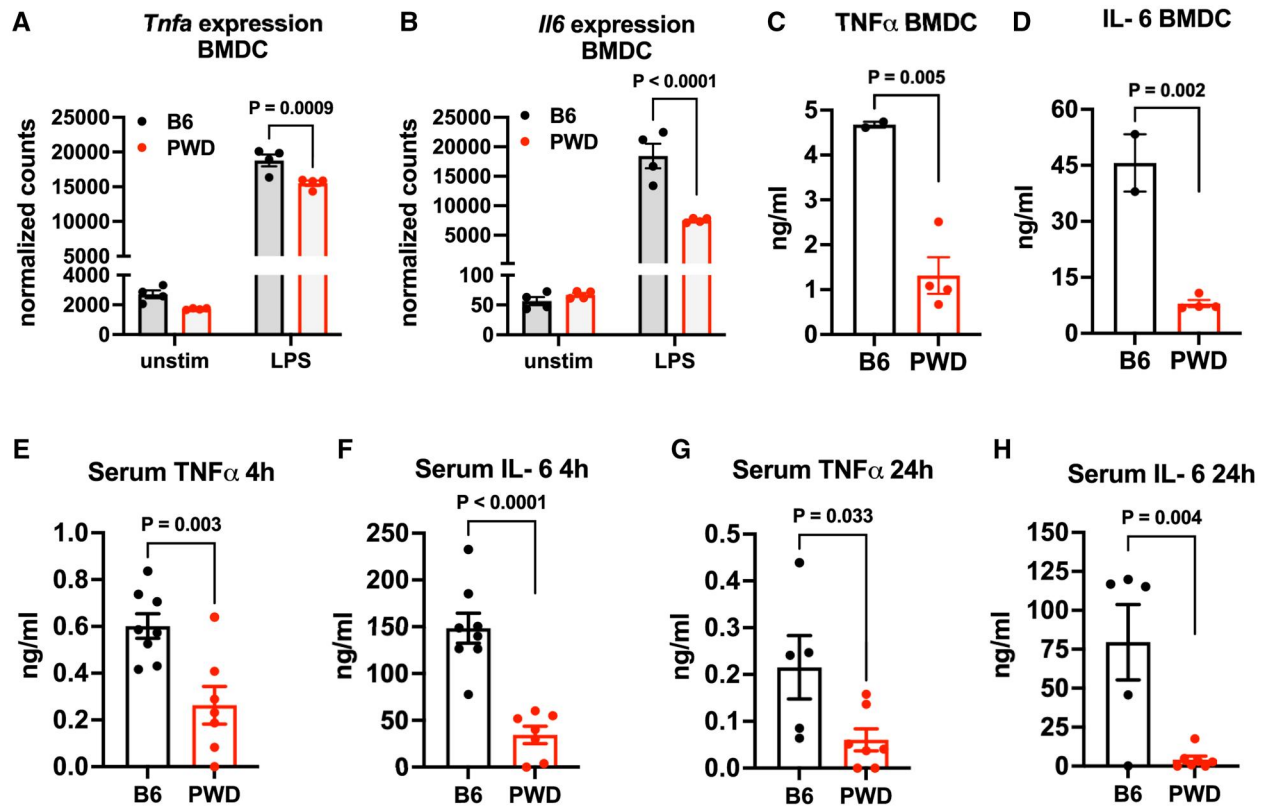


Figure 3. PWD mice produce lower levels of LPS-induced TNF- α and IL-6 compared with B6 mice in vitro and in vivo. (A, B). Normalized counts of *Tnfa* and *Il6* genes were extracted from RNA-seq analysis shown in Fig. 1. (C, D) B6 and PWD BMDCs were stimulated with LPS (10 ng/ml) for 24 h and supernatants were collected, followed by ELISA analysis for TNF- α and IL-6 cytokines in C and D, respectively. (E–H) B6 (n = 8, 4M and 3F) and PWD (n = 7, 3M and 4F) mice were challenged with 20 mg/kg of LPS per mouse i.p., and blood was collected at 4 hrs (E, F) and 24 hrs (G, H), followed by measurement of TNF- α and IL-6 by ELISA. For statistical analyses in A and B, we used two-way ANOVA and Sidák test for post-hoc pairwise comparisons. For other panels, unpaired t test was used to compare between two groups, with P values indicated in each figure panel.

BMDCs compared to B6, which was in fact more pronounced than the differences in mRNA levels (Fig. 3C, D). Next, we assessed systemic cytokine levels in B6 and PWD mice during LPS endotoxemia, which could contribute to differential clinical responses in these mice observed in Fig. 1. B6 and PWD mice were challenged with a sublethal dose of LPS, followed by collection of serum at 4 h and 24 h post-injection and analysis of TNF- α and IL-6 levels by ELISA. Mirroring the in vitro BMDC data, we found significantly reduced amounts of systemic TNF- α and IL-6 in PWD mice at both the time points (Fig. 3E–H). These data demonstrate that genetic variation between B6 and PWD mice regulates not only LPS-induced cytokine gene transcription in myeloid cells in vitro, but also cytokine secretion, both in vitro and in vivo, with restrained cytokine production driven by the PWD genotype correlating with improved clinical outcomes.

Sex modulates transcriptional responses in a genotype-dependent manner

In our previous studies, we have shown the sex by genotype interactions are important in regulating transcriptional and phenotypic responses in genetically diverse mice, under homeostatic conditions or during infection or autoimmunity.^{13,17,22,40} Here, given the protective effect of male sex observed in our in vivo endotoxemia model (Fig. 1I–K), we investigated the role of sex in the regulation of transcriptional responses in myeloid cells stimulated by LPS in naturally divergent B6 and PWD mice. Since the BMDC RNA-seq experiment included cells isolated from both sexes ($n=2$ per sex for each genotype), pooled sex data presented in Fig. 2 was reanalyzed for effects of sex. First, we combined samples independent of treatment (i.e. LPS-treated and untreated), and performed differential gene expression analysis comparing females to males within each genotype (Fig. 4A–C). Since sex effects on gene expression can often result in significant changes of smaller magnitude,⁴¹ we used a cutoff of $P_{adj} < 0.05$, but without a fold-change cutoff. We identified 27 and 25 DEGs, in B6 and PWD BMDCs, respectively; with Y-linked genes and the female-specific X-inactivation gene *Xist* and showing the most significant changes, as expected (Fig. 4A, B; File S2). Eleven of the DEGs were encoded on the X and Y chromosomes, where 6 were shared between genotypes (predominantly Y genes), and 5 genes were unique to each (predominantly X genes) (Fig. 4C; File S2). Some of the X-encoded genes in were among those genes known to escape X inactivation,^{41,42} including *Eif2s3x*, *Kdm6a*, with higher expression in females compared with males (File S2). Interestingly, more than half of sex-biased DEGs was encoded on the autosomes, with the majority of these genes unique to each genotype, with only 1 gene in common (Fig. 4C). These data indicate that sex differences in transcriptional responses in B6 and PWD BMDCs comprise genes encoded both by the sex chromosomes and the autosomes, with many sex differences unique to each genotype.

Given our interest in transcriptional differences during inflammation, we next assessed the effect of sex in the subset of samples that had undergone LPS stimulation. Differential gene expression between female and male LPS-activated BMDCs was assessed within each genotype (Fig. 4D–F). For volcano plots, we excluded the most highly significant X and Y-linked genes from the plots to better visualize the remaining genes (Fig. 4D, E). We found a total of 10 sex-biased genes encoded on the X and Y chromosomes, where 9 of

them shared between B6 and PWD. However, the majority of the sex-biased DEGs were in fact encoded on the autosomes and were unique to B6 or PWD, with 87 and 55 DEGs, respectively, and only 5 genes in common (Fig. 4F). To reveal the distinct biological processes involved in male or female-biased genes, we subjected sex-biased DEGs unique to each genotype to GO pathway enrichment analysis (Fig. 4G, H). Here, we found that female-biased genes in B6 BMDCs were associated with immune response pathways, for example, *immune system process*, *response to stress*, and *response to external stimulus*, including *Il6*, *Vcam1*, *Marco*, *Iigp1*, *Cxcl9*, *Il12rb2*, and *Ear2* (Fig. 4G and File S2). Conversely, we found that male-biased genes in B6 BMDCs were associated with more regulatory pathways important for immune homeostasis, for example, *regulation of lymphocyte proliferation*, *negative regulation of cell population proliferation*, and *regulation of leukocyte activation*, including *Havcr2*, *Gpnmb*, *Mmp9*, *Il4i1*, *Tnfrsf9*, *Il2ra*, *Pgf*, and *Ido1* (Fig. 4G and File S2). Similar to the findings in B6, we found that female-biased DEGs in PWD BMDCs were associated with the immune response pathways such as *defense response to other organism*, *cellular response to chemical stimulus* and *response to stress*, involving candidate genes like, *Lcn2*, *Ciita*, *F5*, *Timp1*, *Ngp*, *Arrb1*, and *Il21r* (Fig. 4H and File S2). Furthermore, male-biased DEGs in PWD BMDCs were associated with cellular processes more related to homeostasis, such as *intracellular zinc ion homeostasis*, *actin-mediated cell contraction*, and *negative regulation of cellular process*, including *Ch25h*, *Pdpr*, *Atp13a2*, *Lmna*, *Ear2*, *Mt1* and *Kdm5d* (Fig. 4H and File S2). Taken together, these data suggest that sex significantly modulates inflammatory transcriptional responses in a genotype-specific fashion. Importantly, while individual sex-biased genes vary greatly by genotype, at the functional level, female transcriptional responses are biased towards proinflammatory processes, which is fully in line with significantly higher mortality and morbidity observed in females during endotoxemia in vivo (Fig. 1).

PWD-derived allelic variants impact transcriptional regulation in cis and trans, driven by transcription factor activity

B6 and PWD genomes differ by a very large number of allelic variants, many of which could contribute to differential transcriptional responses between activated B6 and PWD myeloid cells in a myriad ways that are difficult to assess mechanistically. As a more tractable model to dissect trans and cis regulation of LPS-induced gene expression by natural genetic variants, we utilized a sub-consomic (partial chromosome substitution) mouse strain carrying a ~50 Mb interval on chromosome (Chr) 11 derived from PWD, on an otherwise completely B6 background, called B6.Chr11.2^{PWD} mice,⁴³ abbreviated here as Chr11.2. The PWD-derived interval on Chr11 in Chr11.2 mice spans from 43.8 Mb to 99.7 Mb, harboring ~1,657 genes, and 952 of them are protein-coding (Fig. 5A and File S3). We previously used the Chr11.2 strain to determine the role of a specific candidate gene, *Nos2*, encoded in this locus, in regulating post-activation mitochondrial metabolism and survival in BMDCs.¹⁵ BMDCs were isolated from B6, PWD, and Chr11.2 mice, and stimulated or not by LPS for 6 h, followed by RNA extraction and RNA-seq analysis (Files S1 and S3). Principal component analysis demonstrated distinct sample clustering based on genotype and treatment, where Chr11.2 samples clustered closer to B6

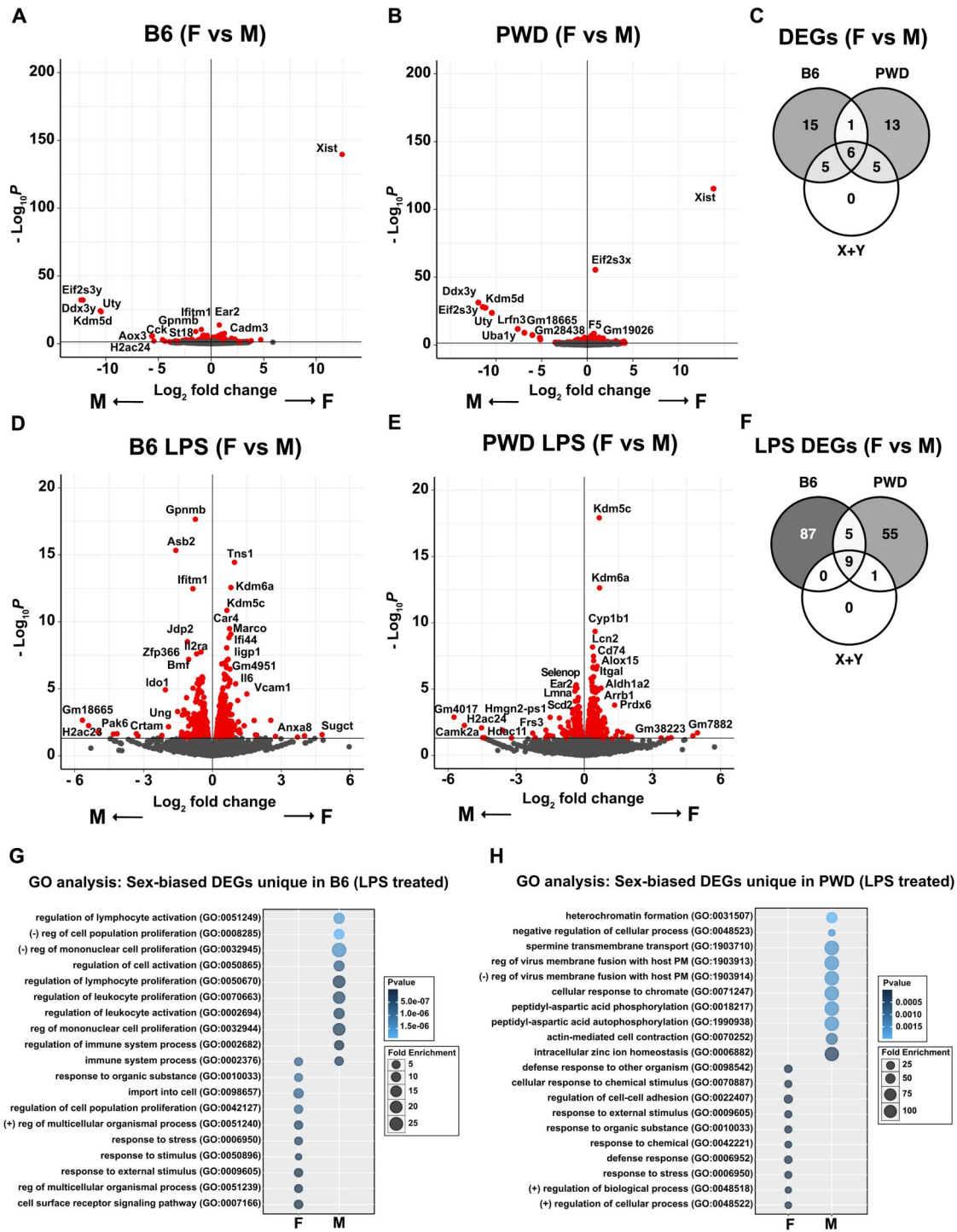


Figure 4. Sex regulates inflammatory transcriptional responses in a genotype-dependent manner. RNA-seq data described in the Fig. 2 were reanalyzed for the effect of sex within B6 (M = 2, F = 2) and PWD (M = 2, F = 2) BMDCs. A cutoff of $P_{adj} < 0.05$ was used to identify DEGs. (A, B) Volcano plots are showing sex-biased DEGs (female vs male) as identified by combining unstimulated and LPS-stimulated B6 or PWD BMDC, in panels A and B, respectively. The most significant genes are labelled by the enhanced volcano tool. (C) Venn diagram depicting overlap between B6 and PWD sex-biased DEGs, indicating the DEGs encoded on the X and Y chromosomes. Here, “X + Y” represents the combined DEGs encoded on the X and Y chromosome in either B6 or PWD BMDC. (D, E) Volcano plots showing sex biased DEGs (female vs male) in LPS-treated B6 or PWD BMDCs, in panel D and E, respectively. To facilitate visualization, the X and Y axes have been adjusted to xlim (–6, 6) and ylim (0, 20) intentionally excluding several of the most highly differentially expressed X and Y chromosomal genes with extremely high significance or fold-change values. The most significant genes are labelled by the enhanced volcano tool. (F) Venn diagram showing the relationship between sex-biased DEGs in B6 and PWD, and X- and Y-linked genes, as in panel C. (G, H) DEGs with female- or male-biased expression in LPS-treated B6 (G) or PWD (H) BMDCs were assessed by GO pathway enrichment analysis using PANTHER. Top 10 pathways in females and males based on P-values are shown for each genotype.

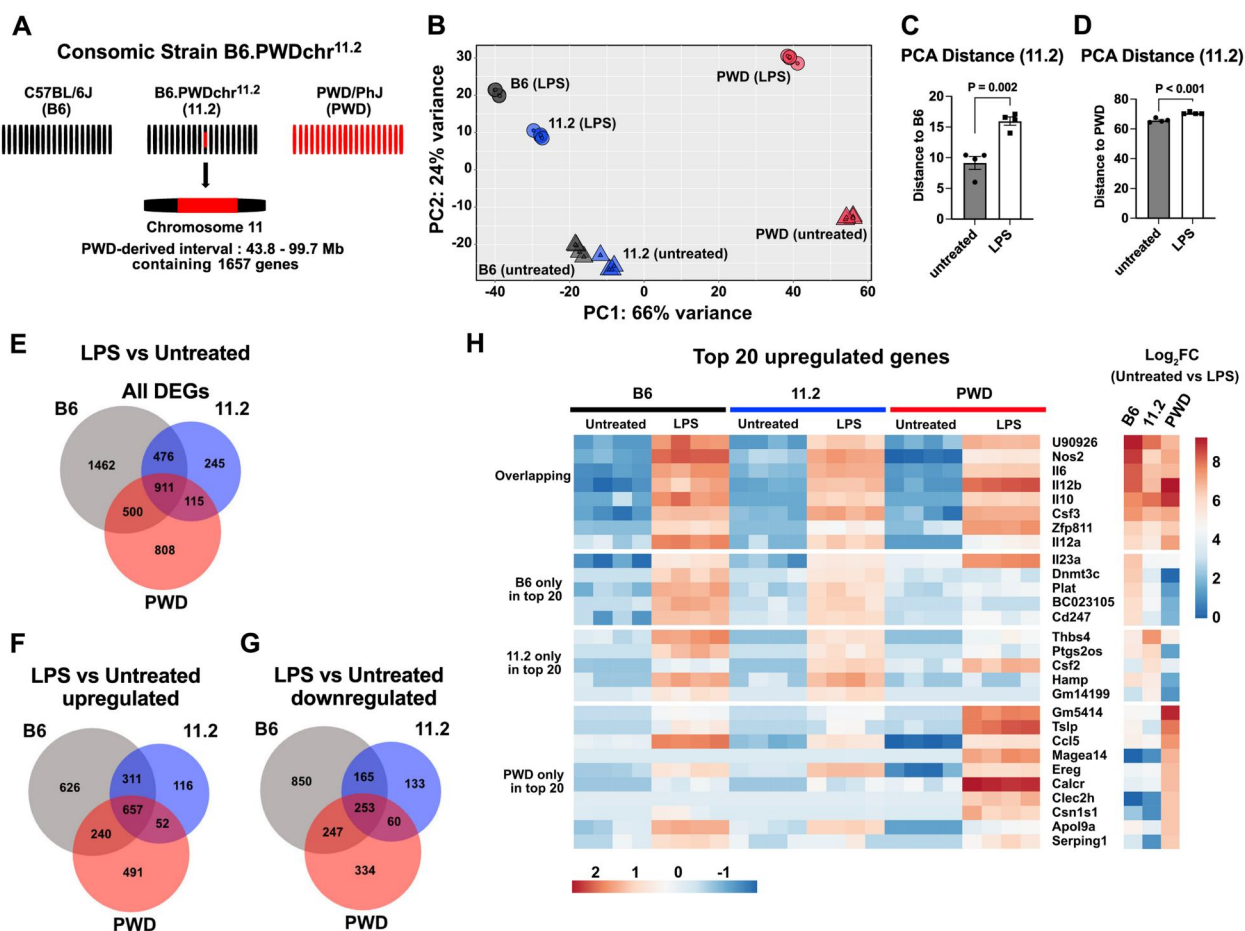


Figure 5. Chr11.2 BMDCs exhibit distinct transcriptional profiles compared with B6 and PWD. BMDCs isolated from B6, Chr11.2 and PWD mice ($n = 4$ in each group; 2 males and 2 females), followed by LPS treatment (10 ng/ml for 6 h) and RNA-seq. DESeq2 analysis was performed to identify genes differentially expressed by LPS treatment for each genotype, using a cutoff of $P_{adj} < 0.05$ and $|\log_2(\text{Fold Change})| \geq 1$. (A) Schematic diagram showing the three strains used in this experiment, including the Chr11.2 and the PWD-derived interval on Chr11. (B) Principal component analysis (PCA) of the RNA-seq data demonstrating clustering of individual samples by genotype and treatment, as annotated. (C, D) PCA coordinate distance from individual Chr11.2 samples to the mean position of B6 (C) or PWD (D) samples was determined for untreated and LPS treated samples, and significance of differences assessed by Student t test. (E–G) Venn diagrams comparing LPS-dependent DEGs in B6, Chr11.2 and PWD BMDCs, subsetted to upregulated and downregulated DEGs in F and G, respectively. (H) Expression of the top 20 (by fold change) LPS-upregulated DEGs for each genotype are represented as a heatmap. DEGs are grouped on the heatmap by showing the overlapping top 20 DEGs between all the three strains first, followed by the unique top 20 DEGs belonging to each strain in the individual top 20 genes. LPS-induced \log_2 fold change for each DEG in all three strains is shown in a heatmap on the right-side panel.

samples than to the PWD samples (Fig. 5B), as expected, considering the majority of this strain's genome is B6-derived. Interestingly, dissimilarity between Chr11.2 and B6, and Chr11.2 and PWD, as assessed by distance on the ordination plot, increased significantly after LPS treatment (Fig. 5C, D). These data suggest that Chr11.2 BMDCs, compared with those of parental B6 and PWD strains, exhibit a unique transcriptional signature that becomes more divergent upon LPS exposure.

Next, we performed differential gene expression analyses using DESeq2, comparing untreated and LPS-treated BMDCs within each genotype. A large number of DEGs were found to be up- and downregulated by LPS treatment in each genotype, with a large number (911) of these conserved between the three genotypes (Fig. 5E–G), comprising a core set of LPS-regulated genes. Expectedly, besides the core shared genes, Chr11.2 had more LPS-induced genes in common with B6 (476 genes) compared those in common with PWD (115 genes); with 245 genes that were unique to Chr11.2 alone (Fig. 5E). Subsetting the DEGs into upregulated and

downregulated categories revealed a similar trend (Fig. 5F, G). To visualize the most highly upregulated genes and assess whether they differ by genotype, we selected the top 20 LPS-upregulated genes (by fold change) from each genotype and compared their expression across the three genotypes (Fig. 5H). Shared upregulated genes included known canonical inflammatory response genes such as *Il6*, *Il10*, *Il12b*, and *Nos2*, and, interestingly, *U90926* (Fig. 5H), a putative lncRNA we recently described as highly inducible by inflammatory signals in myeloid cells, which functions as a negative regulator of septic shock.²⁵ A number of top upregulated genes for B6 or Chr11.2 BMDCs shared a similar pattern with one another, but had minimal induction in PWD, such as *Cd247* and *Ptgs2os*; while the converse was true for many of the top upregulated genes in PWD, like *Tslp*, *Calcr*, and *Ereg*, which lacked induction in B6 or Chr11.2 (Fig. 5H). Together, these data suggest PWD-derived allelic variants in the Chr11.2 interval regulate proinflammatory transcriptional responses and capture a subset of divergent transcriptional responses seen in PWD cells.

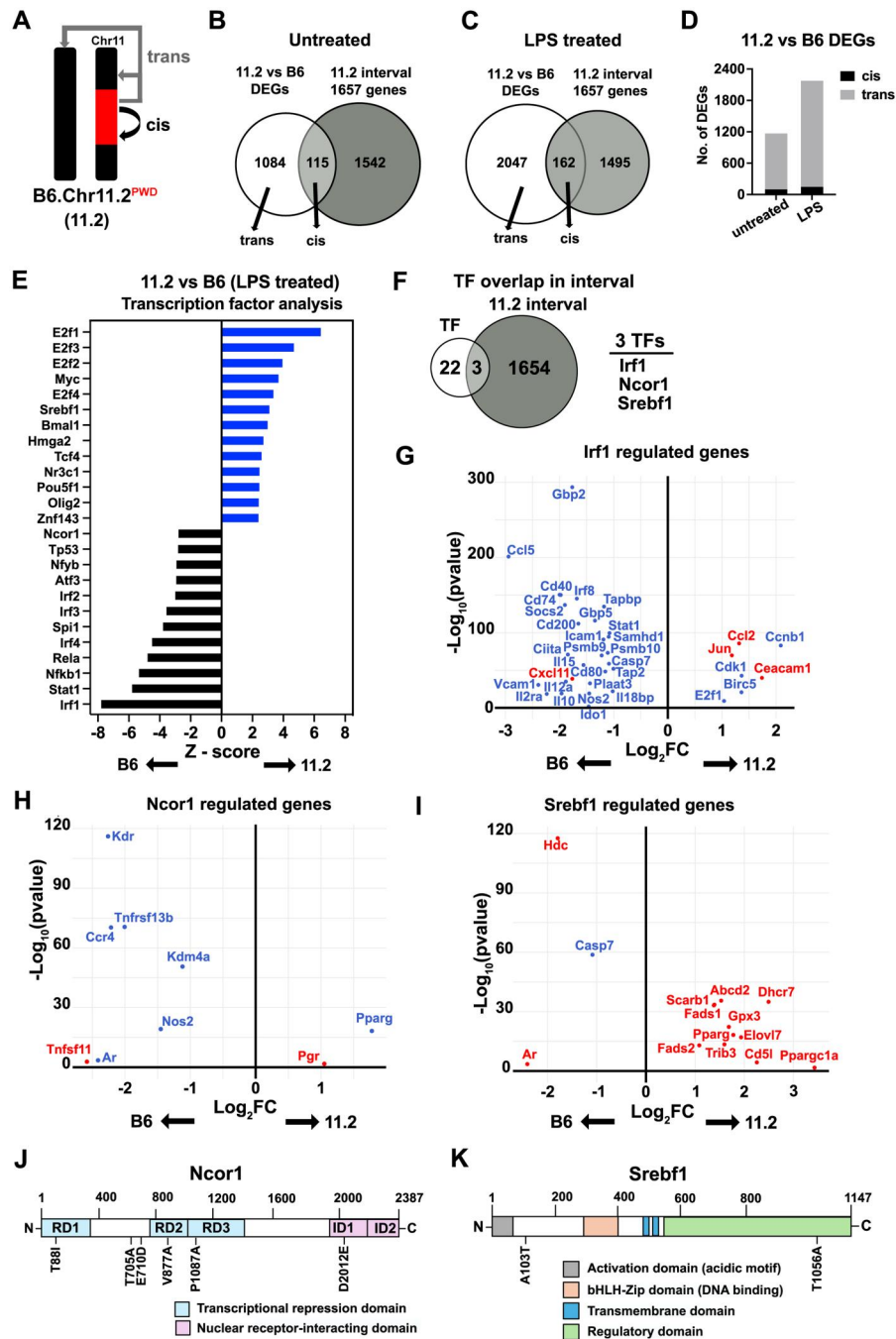


Figure 6. PWD allelic variants encoded in the Chr11.2 interval modulate LPS-stimulated transcriptional responses in cis and in trans via modulation of transcription factor activity. (A) Schematic representation of cis and trans regulation by variants in the Chr11.2 interval. (B, C) RNA-seq data generated as in Fig. 5, was analyzed by DESeq2 to directly compare Chr11.2 and B6 genotypes within untreated and LPS-treated samples. A cutoff of $P_{adj} < 0.05$ and $|\text{Log}_2\text{Fold}| \geq 1$ was used to identify DEGs, with a positive fold change indicating increased expression in Chr11.2 relative to B6. Venn diagrams comparing DEGs from Chr11.2 vs B6 analysis to the 1,657 genes encoded in the Chr11.2 interval, in untreated (B) and LPS-treated (C) groups, with cis and trans DEGs indicated. (D) Number of cis and trans DEGs in untreated and LPS-treated conditions. (E) DEGs from LPS-treated samples were analyzed by *decoupleR* to predict enriched TFs and infer their activity. Top 25 TFs based on Z score (both directions) regulating DEGs are shown in panel E, where blue and black bars indicate increased TF activity in Chr11.2 or B6, respectively. (F) Venn diagram showing the overlap between top 25 TFs and the total 1,657 genes encoded in the Chr11.2 interval, with the three overlapping genes indicated to the right. (G–I) Three TFs encoded in the Chr11.2 interval were analyzed to visualize the differential expression of their target genes between Chr11.2 and B6 BMDCs. Irf1, Ncor1 and Srebf1 regulated genes in the LPS-treated DEGs (11.2 vs B6) are shown in panels G, H and I, respectively. Blue indicates “known” negative regulation by the TF and red indicates positive regulation. Fold change represents the expression of the DEG in Chr11.2 relative to B6, with positive indicating higher expression in Chr11.2. (J, K) Schematic diagrams showing Ncor1 and Srebf1 functional domains and positions of the coding non-synonymous single nucleotide polymorphisms (nsSNPs) distinguishing PWD (as surrogate for PWD) and B6 alleles (see Methods).

Allelic variants in gene promoter or proximal enhancer variants typically regulate the expression of proximal genes in cis. In contrast, trans regulation of expression by allelic variants involves more complex mechanisms, including

variants that modify distal enhancers, inter/intra-chromosomal interactions, or pleiotropically acting genes, such as transcription factors. Transcriptional profiles of Chr11.2 BMDCs provided a model to investigate the

mechanisms driving such cis or trans regulation by PWD-derived allelic variants. We designated the genes encoded by PWD-derived interval on Chr11 in Chr11.2 mice (1,657 genes) as cis, and any genes outside the interval as trans (Fig. 6A). To identify genes whose expression was regulated by the variants in Chr11.2 interval, we performed differential expression analysis comparing Chr11.2 to B6 BMDCs, either untreated or LPS-treated samples, and determined whether the DEGs fell into the cis or trans category. Approximately 7% to 10% of all Chr11.2 DEGs were cis genes, with 115 cis genes and 1,084 trans genes in the untreated condition and 162 cis genes and 2,047 trans genes in the LPS-treated condition (Fig. 6B, C). The total number of Chr11.2-specific DEGs was higher in LPS-treated samples compared to untreated samples, with an increased proportion (from 90 to 93%) of trans DEGs (Fig. 6D). These data suggest that the PWD-derived allelic variants encoded by the interval in Chr11.2 mice robustly regulate gene expression in trans, with a stronger effect observed after BMDC activation.

A plausible mechanism for trans regulation by allelic variants is differential regulation of transcription factor (TF) activity, either through differential expression of the TF(s) themselves, or coding variants that impact TF function. To test these hypotheses, we first used Chr11.2-specific DEGs to infer in an unbiased manner the altered activity of specific TFs using the *decoupleR* package, which measures relative enrichment and directionality of gene expression of known TF target genes within a gene set.²⁹ This identified a number of TFs with inferred activity that was either increased in Chr11.2 BMDCs or decreased in Chr11.2 BMDCs (ie increased in B6) (Fig. 6E). We compared the top 25 predicted TFs (File S4) with the 1,657 genes in the PWD interval of Chr11.2 mice to determine if any of the TFs are encoded within that region. We found 3 of these TFs, *Irf1* (interferon regulatory factor 1), *Ncor1* (nuclear receptor co-repressor 1) and *Srebf1* (sterol regulatory element-binding transcription factor 1), encoded in the Chr11.2 interval (Fig. 6F). Analysis of expression of known TF target genes in our DEGs set (11.2 vs B6) from LPS-stimulated samples (see Methods) identified key targets and confirmed inferred directionality of TF activity, with *Irf1* and *Ncor1* exhibiting reduced activity in Chr11.2 BMDCs, and *Srebf1* exhibiting enhanced activity (Fig. 6G–I). To determine mechanisms by which these transcription factors could be affecting gene regulation, we first assessed whether these TFs were differentially expressed in Chr11.2 BMDCs, and found that *Irf1*, *Ncor1* and *Srebf1* were not differentially expressed at baseline or after LPS stimulation, in comparison with B6 BMDCs (File S3). Next, because protein coding variants can profoundly impact gene function, we examined the presence of non-synonymous single nucleotide polymorphisms (nsSNPs) in the genes encoding these TFs, distinguishing B6 and PWD alleles (using PWK genome sequencing data as a surrogate for PWD; see Methods). We found that two out of the three TFs, *Ncor1* and *Srebf1* had six and two nsSNPs, respectively, which we mapped to functional domains (see Methods) (Fig. 6J, K). We found that in *Ncor1*, three nsSNPs are situated within transcriptional repression domains, and 1 nsNP is in the nuclear receptor-interacting domain (Fig. 6J). We also found that 1 out of the 2 nsSNPs of *Srebf1* is located in the regulatory domain (Fig. 6K). These data identify candidate polymorphisms in the functional domains of *Ncor1* and *Srebf1* that could be responsible for driving differential gene regulation in Chr11.2 strain in trans. Taken together, our data suggest that naturally occurring genetic variants can

robustly regulate myeloid cell inflammatory gene expression in cis and in trans, with the latter likely driven by polymorphism-dependent differential transcription factor activity.

Discussion

Genome wide studies in humans have begun to identify genetic determinants of sepsis outcomes, but with limited success so far.^{44,45} Animal models of sepsis and associated inflammatory responses have the potential to provide important mechanistic insights into human disease, but the vast majority of such studies have utilized models of limited genetic diversity—as these studies are typically performed in B6 mice and other common laboratory strains—a potential blind spot. Here, we utilized the genetic diversity and evolutionarily relevant genetic variation naturally occurring in wild-derived mice to assess how genetic variation controls physiologic and transcriptional responses to endotoxemia. Compared with B6 mice, wild-derived PWD mice exhibited restrained inflammatory responses and reduced morbidity and mortality in vivo. In vitro, myeloid cell responses to endotoxin stimulation revealed both unique and conserved transcriptional programs in PWD mice. Using a subconsomic strain carrying a portion of the PWD genome, we were able to demonstrate cis and trans regulation of transcriptional responses and identify candidate trans regulators as transcription factors IRF-1, NCOR1, and SREBF1.

We found that PWD mice are markedly resistant to challenge with systemic LPS, with minimal clinical signs and rapid recovery at doses that were lethal to 85% of the B6 mice. This was paralleled by reduced acute stage peak cytokine production in the serum at 4 h post challenge, and rapid resolution of hypercytokinemia by 24 h. A simple explanation for this divergent phenotype could be a defective allele(s) controlling TLR4 signaling, analogous to the classic example of defective variants in *Tlr4* identified in endotoxin-shock resistant C3H/HeJ mice,⁴⁶ or the reverse example of hypomorphic variants in anti-inflammatory genes *Irak2* and *Irak1bp1* that promote TLR activation in MOLF/Ei mice, a different wild-derived strain that is hypersusceptible to sepsis.^{47,48} Arguing against this possibility, a previous study has documented that the *Tlr4* allele from PWK/PhJ mice, which are very closely related to PWD, is normally functional despite the presence of a number nsSNPs.⁴⁹ Moreover, while we have not formally assessed all of the major downstream components of TLR4 signaling in PWD mice, the robust *in vitro* transcriptional responses elicited by LPS stimulation in PWD BMDCs, including the strong upregulation of many canonical genes like *Il12a*, *Il12b*, *Il10*, and *Nos2* (e.g. Figs 2C and 5H), argue against the scenario under which a hypomorphic PWD allele would be simply dampening TLR4 signaling. Instead, rather than a quantitative decrease in the magnitude of the LPS response in PWD, we found that this response was qualitatively different, with a unique gene signature and distinct biological pathways, in addition to the partially shared stereotypical B6-like response. Furthermore, the finding that a PWD-derived interval on Chr11, which does not encode any known major TLR4 signaling components (File S3), still captured a significant number of PWD-specific LPS induced genes, also argues against this possibility. Therefore, we believe that this divergent response is driven by a complex combination of genetic variants that regulate gene expression in cis (e.g. promoter variants driving differential TF binding)

and in trans (e.g. TFs with different activities due to coding variants). We provide evidence in Chr11.2 subconsomic mice to support both mechanisms. Nonetheless, future studies will need to also assess induction of canonical signaling components downstream of TLR4 and other TLRs in PWD myeloid cells. Another important limitation of our study is the use of LPS-stimulated BMDCs as an in vitro model of transcriptional responses in sepsis, as these cells likely do not fully recapitulate the in vivo sepsis response of key myeloid cells like Kupffer cells, monocytes, or neutrophils. Future studies could extend our findings via transcriptional analysis of in vivo-activated myeloid cells isolated from LPS-challenged mice.

It is of note that while wild-derived PWD mice are resistant to a number of inflammatory pathologies, including autoimmune demyelination and inflammatory bowel disease,^{17,18,50} and yet also control viral infection better compared with B6 mice.^{13,51} Future studies will need assess the susceptibility of PWD mice to bacterial sepsis, where the balance of protective and deleterious inflammatory and antimicrobial responses would determine host survival. Another strikingly similar example is the resistance to LPS- or TNF-induced shock and bacterial sepsis observed in SPRET/EiJ wild-derived mice.²¹ Altogether this suggests that rather than having a broadly dampened immune response, many (though not all; see the example of MOLF/EiJ mice above) strains of wild-derived mice have superior immunoregulatory capacity. Our transcriptional profiling suggests that this is driven by simultaneous upregulation of anti-inflammatory or tissue protective genes in PWD, e.g. *Tgfb2*, *Arg2*, *Tslp*, *Ereg*, *Calcr*, and others (Figs 2B and 5H, File S1). It is tempting to speculate that the lack of evolutionary pressure exerted by infectious agents on B6 and other laboratory strains of mice that have been bred in captivity and clean environments for an extended length of time has over time contributed to a loss of immune regulatory capacity, although this is a challenging hypothesis to test. Nonetheless, our results sound a cautionary note regarding (over)interpretation of experimental findings in classic inbred laboratory mice, and support a broader approach including more diverse genotypes in pre-clinical and experimental research, to enhance translatability to genetically diverse human populations, and to facilitate the discovery of novel regulatory mechanisms. More specifically, we suggest that investigators that have made key pre-clinical observations using B6-like classic strains should validate those findings in 2-3 commercially available wild-derived strains, such as PWD, PWK, or WSB, prior to proposing to advance their preclinical findings to human trials. Using multiple strains to validate their findings can elucidate a common axis for therapeutic targeting to achieve maximal response rates in genetically diverse human populations.

Another unique feature of the transcriptome of activated PWD myeloid cells was the expression of a number of transcripts annotated as pseudogenes in the reference (B6-based) genome. In fact, of the top 40 genes most highly (by fold change) overrepresented in PWD vs B6 activated BMDCs, only 15 were protein-coding, while 21 were pseudogenes, 2 were ribozymes, and 1 was a lncRNA (File S1). Similarly, of the total 746 pseudogenes differentially expressed between PWD and B6 activated BMDCs, 625 were overrepresented in PWD and only 121 were overrepresented in B6 (File S1). This suggests that many of the genes annotated as pseudogenes based on the well-characterized B6 genome may in fact represent functional genes in the divergent PWD genome, and their

function should be deciphered in future studies. Additionally, numerous (544) lncRNA genes were differentially expressed between PWD and B6 activated BMDCs. However, we saw no overall bias in expression between genotypes, with 284 lncRNA genes overrepresented in B6 and 260 overrepresented in PWD, suggesting the existence of unique lncRNA profiles in both genotypes. Interestingly, *Ptgs2os2* (encoding the well characterized LPS-inducible linc-Cox2 gene^{52,53} and the neighboring *Ptgs2os* gene were strongly overrepresented ($\log_2(\text{FC}) > 2.5$ and 3.31, respectively) in B6 BMDCs (File S1), suggesting genotype-specific regulation of these lncRNAs, which were originally identified and characterized in B6 mice. In contrast, the putative lncRNA *U90926* was among the top LPS-upregulated genes in all genotypes. These results suggest that non-coding genes and pseudogenes could represent an important and mostly unexplored layer of transcriptional regulation driven by genetic variants.

We used the sub-consomic Chr11.2 strain as a model to assess how allelic variants in a defined region of the genome can impact gene expression in cis and in trans. We found that the PWD-derived locus on Chr11 regulated the expression of a large number of genes in other regions of the genome. In search of a potential trans mechanism, we used bioinformatics to infer differential TF activity, identifying 3 TFs (*Irf1*, *Ncor1*, and *Srebf1*) encoded in this locus as candidate trans regulators. *Ncor1*^{PWD} and *Srebf1*^{PWD} alleles contained nsSNPs in regulatory or effector domains, providing a potential mechanism for allele-specific differential activity. The mechanism underlying the (inferred) reduced activity of *Irf1*^{PWD} is unclear, but could involve alternative splicing, posttranscriptional regulation, and/or differential activation by upstream signals. We acknowledge that besides TF activity, there are a number of other potential trans regulators, including signaling molecules integrating inflammatory signals such as kinases, rapidly released cytokines that could result in autocrine feedback, or enzymes that generate effector molecules that modulate cell state and gene expression. With regard to the latter, we have previously used Chr11.2 mice to determine the role of a specific candidate gene, *Nos2*, encoded in this locus, in regulating post-activation mitochondrial metabolism and survival in BMDCs.¹⁵ We note that the effects exerted by the *Nos2*^{PWD} allele were post-transcriptional and mainly observed after 24 h of LPS stimulation,¹⁵ and thus are likely exhibiting minimal effects in our acute model of LPS activation used here. Notably, the Glass group recently performed deep genomic profiling of bone marrow-derived macrophages (BMDM) derived from 5 genetically diverse mouse strains, including B6 and PWK/PhJ.¹⁶ In agreement with our findings, they found that wild-derived genotypes exerted profound effects on gene expression through differential TF activity and cis and trans regulatory effects. Interestingly, through the use of inter-strain F1 hybrids and assessment of allele-specific expression, they demonstrated that ~80% of allele-specific gene expression in F1 heterozygous BMDM occurred in cis rather than in trans, which is contrasted by our results in the Chr11.2 model, where ~90% of DEGs were regulated in trans. This likely reflects the genetic differences between these 2 distinct models, which has interesting implications for mechanisms by which allelic variants could regulate gene expression. One potential mechanism is the existence of so-called expression quantitative trait loci (eQTL) “hotspots” in specific regions of the genome. Such “hotspots” regulate large numbers of

genes in trans,^{54,55} and it is likely that an immune cell-specific eQTL “hotspot” could be localized to the Chr11.2 locus. The availability of immune-specific eQTL data from genetic reference populations such as the Diversity Outbred mice⁵⁶ could facilitate such discoveries in the future.

Sex differences in sepsis outcomes and associated inflammatory responses have been well documented in human studies and animal models.⁵⁷ Our studies revealed sex differences in endotoxic shock outcomes *in vivo*, as well as transcriptional differences *in vitro*. In *in vivo*, female mice exhibited significantly higher morbidity and/or mortality, independent of strain. While this appears to be in contrast with studies in humans, where females have favorable sepsis outcomes compared with males,⁵⁷ this likely represents stronger inflammatory responses in females that are detrimental in the LPS shock model, but protective in promoting a stronger antimicrobial response during sepsis. Interestingly, while the effect of sex was phenotypically similar in both PWD and B6 mice *in vivo*, the transcriptional differences between male and female BMDCs were markedly divergent by genotype, with the exception of Y-linked and several X-linked genes (Fig. 4C and F). This suggests the existence of genotype-by-sex interactions driving differential transcriptional responses in activated myeloid cells. Interestingly, pathway enrichment analysis of female- and male-biased genes revealed that despite divergence in individual gene identities, the functional profile of female-biased genes was skewed toward pro-inflammatory pathway activation in both genotypes, which is congruent with the similarity of biological outcomes *in vivo*. While future studies could define the mechanisms driving these sex differences (e.g. influence of sex chromosomes vs. sex hormones), it is notable that they persist in the BMDC model despite 7 day-long culture of cells *ex vivo* in standard media, which may contain estrogenic compounds. Taken together, our results confirm that female sex drives a stronger proinflammatory response during endotoxemia but suggest that the molecular mechanisms underlying such sex differences likely differ across genotypes, arguing against a one-size-fits-all therapeutic approach tailored to one sex.

Our results, together with previous studies from others (discussed above), demonstrate that natural genetic variation in mice exerts a profound influence on susceptibility to endotoxic shock and myeloid cell transcriptional responses to endotoxin. By extension, this implies that genetic variation in humans likely influences heterogeneous outcomes in sepsis via similar mechanisms. This could have important implications for the development of personalized interventions for this often-fatal condition, as well as predictive algorithms and biomarkers for risk stratification. Given the challenges and confounders faced by sepsis GWAS in humans, including large variability in patient comorbidities and other non-genetic predisposing factors, forward genetic screens in genetically diverse mouse populations, such as the Collaborative Cross or the Diversity Outbred, provide a cost-effective alternative to determine the genetic basis of sepsis susceptibility. We believe that such studies in the future, when properly integrated with emerging sepsis GWAS in humans, can provide important biological insights.

Acknowledgments

The authors thank the following UVM core facilities and their staff for providing invaluable technical support: Flow

Cytometry and Cell Sorting Facility and the Vermont Integrative Genomics Resource for RNA sequencing and analysis.

Author contributions

B.S., J.P.S., E.A., S.E.F., and D.N.K. conceived the study and designed experiments. B.S., J.P.S., and K.J.S. performed the experiments. B.S., J.P.S., S.E.F., P.D.R., and D.N.K. analyzed the data. E.A. and D.N.K. secured funding to support the experiments.

Supplementary material

Supplementary material is available at *ImmunoHorizons* online.

Funding

The study was supported by the following grants: R01AI172166 from the NIH/NIAID to DNK, 5T32AI055402-08 from the NIH/NIAID (PI: Gary Ward), and P30GM118228 from NIH/NIGMS (PI: Ralph Budd).

Conflicts of interest

None declared.

Data availability

The data underlying this article are available in the article and in its online supplementary material. The RNAseq data are available in GEO repository, under GSE272206.

References

1. Rudd KE et al. Global, regional, and national sepsis incidence and mortality, 1990–2017: analysis for the Global Burden of Disease Study. *Lancet*. 2020;395:200–211.
2. Caraballo C, Jaimes F. Organ dysfunction in sepsis: an ominous trajectory from infection to death. *Yale J Biol Med*. 2019; 92:629–640.
3. Raymond SL et al. Microbial recognition and danger signals in sepsis and trauma. *Biochim Biophys Acta Mol Basis Dis*. 2017; 1863:2564–2573.
4. Ozment TR et al. Scavenger receptor class a plays a central role in mediating mortality and the development of the pro-inflammatory phenotype in polymicrobial sepsis. *PLoS Pathog*. 2012; 8:e1002967.
5. Deitch EA. Rodent models of intra-abdominal infection. *Shock* 2005;24(Suppl 1):19–23.
6. Khan HN et al. Leukocyte transcriptional signatures dependent on LPS dosage in human endotoxemia. *J Leukoc Biol*. 2019; 106:1153–1160.
7. Medzhitov R, Horng T. Transcriptional control of the inflammatory response. *Nat Rev Immunol*. 2009;9:692–703.
8. Gong T, Liu L, Jiang W, Zhou R. DAMP-sensing receptors in sterile inflammation and inflammatory diseases. *Nat Rev Immunol*. 2020;20:95–112.
9. Fink MP. Animal models of sepsis. *Virulence*. 2014;5:143–153.
10. Zanotti-Cavazzoni SL, Goldfarb RD. Animal models of sepsis. *Crit Care Clin*. 2009;25:703–719. vii–viii.
11. Dyson A, Singer M. Animal models of sepsis: why does preclinical efficacy fail to translate to the clinical setting? *Crit Care Med*. 2009;37:S30–37.
12. Gregorová S, Forejt J. PWD/Ph and PWK/Ph inbred mouse strains of *Mus m. musculus* subspecies—a valuable resource of

- phenotypic variations and genomic polymorphisms. *Folia Biol. (Praha)*. 2000;46:31–41.
13. Sabikunnahar B et al. Sex differences in susceptibility to influenza A virus infection depend on host genotype. *PloS One*. 2022; 17:e0273050.
 14. Dupont MSJ et al. Host genetic control of natural killer cell diversity revealed in the Collaborative Cross. *Proc Natl Acad Sci USA*. 2021;118:e2018834118.
 15. Snyder JP et al. Divergent genetic regulation of nitric oxide production between C57BL/6J and wild-derived PWD/PhJ mice controls postactivation mitochondrial metabolism, cell survival, and bacterial resistance in dendritic cells. *J Immunol*. 2022;208:97–109.
 16. Link VM et al. Analysis of genetically diverse macrophages reveals local and domain-wide mechanisms that control transcription factor binding and function. *Cell*. 2018;173:1796–1809.e17.
 17. Bearoff F et al. Natural genetic variation profoundly regulates gene expression in immune cells and dictates susceptibility to CNS autoimmunity. *Genes Immun*. 2016;17:386–395.
 18. Lahue KG et al. Identification of novel loci controlling inflammatory bowel disease susceptibility utilizing the genetic diversity of wild-derived mice. *Genes Immun*. 2020;21:311–325.
 19. Graham JB et al. Extensive homeostatic T cell phenotypic variation within the Collaborative Cross. *Cell Rep* 2017; 21:2313–2325.
 20. Poltorak A, Apalko S, Sherbak S. Wild-derived mice: from genetic diversity to variation in immune responses. *Mamm Genome*. 2018;29:577–584.
 21. Timmermans S et al. Using the inbred mouse strain SPRET/EiJ to provide novel insights in inflammation and infection research. *Mamm Genome*. 2018;29:585–592.
 22. Kremontsov DN, Asarian L, Fang Q, McGill MM, Teuscher C. Sex-specific gene-by-vitamin D interactions regulate susceptibility to central nervous system autoimmunity. *Front Immunol* 2018; 9:1622.
 23. Raza A et al. Anti-inflammatory roles of p38 α MAPK in macrophages are context dependent and require IL-10. *J Leukoc Biol*. 2017;102:1219–1227.
 24. Okeke EB, Okwor I, Uzonna JE. Regulatory T cells restrain CD4+ T cells from causing unregulated immune activation and hypersensitivity to lipopolysaccharide challenge. *J Immunol*. 2014; 193:655–662.
 25. Sabikunnahar B et al. Long Noncoding RNA U90926 Is Induced in Activated Macrophages, Is Protective in Endotoxic Shock, and Encodes a Novel Secreted Protein. *J Immunol*. 2023;210:807–819. [10.4049/jimmunol.2200215](https://doi.org/10.4049/jimmunol.2200215) 36705532
 26. Dobin A et al. STAR: ultrafast universal RNA-seq aligner. *Bioinformatics*. 2013;29:15–21.
 27. Love MI, Huber W, Anders S. Moderated estimation of fold change and dispersion for RNA-seq data with DESeq2. *Genome Biol*. 2014;15:550.
 28. Mi H, Muruganujan A, Casagrande JT, Thomas PD. Large-scale gene function analysis with PANTHER Classification System. *Nat. Protoc*. 2013;8:1551–1566.
 29. Badia-I-Mompel P et al. decoupleR: ensemble of computational methods to infer biological activities from omics data. *Bioinforma Adv*. 2022;2:vbac016.
 30. Mottis A, Mouchiroud L, Auwerx J. Emerging roles of the corepressors NCoR1 and SMRT in homeostasis. *Genes Dev*. 2013; 27:819–835.
 31. Daemen S, Kutmon M, Evelo CT. A pathway approach to investigate the function and regulation of SREBPs. *Genes Nutr*. 2013; 8:289–300.
 32. Yang J, Stack MS. Lipid regulatory proteins as potential therapeutic targets for ovarian cancer in obese women. *Cancers*. 2020; 12:3469.
 33. Wong MM, Guo C, Zhang J. Nuclear receptor corepressor complexes in cancer: mechanism, function and regulation. *Am J Clin Exp Urol*. 2014;2:169–187.
 34. Gandhi R, Hayley S, Gibb J, Merali Z, Anisman H. Influence of poly I:C on sickness behaviors, plasma cytokines, corticosterone and central monoamine activity: moderation by social stressors. *Brain Behav Immun*. 2007;21:477–489.
 35. Lakbar I et al. Interactions between gender and sepsis-implications for the future. *Microorganisms*. 2023;11:746.
 36. Gotts JE, Matthay MA. Sepsis: pathophysiology and clinical management. *BMJ*. 2016;353:i1585.
 37. Peng T, Lu X, Lei M, Moe GW, Feng Q. Inhibition of p38 MAPK decreases myocardial TNF-alpha expression and improves myocardial function and survival in endotoxemia. *Cardiovasc Res*. 2003;59:893–900.
 38. Riedemann NC et al. Protective effects of IL-6 blockade in sepsis are linked to reduced C5a receptor expression1. *J Immunol* 2003; 170:503–507.
 39. Tanaka T, Narazaki M, Kishimoto T. IL-6 in inflammation, immunity, and disease. *Cold Spring Harb Perspect Biol*. 2014; 6:a016295.
 40. Bearoff F et al. Identification of genetic determinants of the sexual dimorphism in CNS autoimmunity. *PLoS One*. 2015; 10:e0117993.
 41. Oliva M, et al. GTEx Consortium The impact of sex on gene expression across human tissues. *Science*. 2020;369:eaba3066.
 42. Xu J, Distech CM. Sex differences in brain expression of X- and Y-linked genes. *Brain Res*. 2006;1126:50–55.
 43. Gregorová S et al. Mouse consomic strains: exploiting genetic divergence between *Mus m. musculus* and *Mus m. domesticus* subspecies. *Genome Res*. 2008;18:509–515.
 44. Hernandez-Beeftink T et al.; Genetics of Sepsis (GEN-SEP) Network. A genome-wide association study of survival in patients with sepsis. *Crit Care*. 2022;26:341.
 45. Engoren M et al. Genetic variants associated with sepsis. *PloS One*. 2022;17:e0265052.
 46. Qureshi ST et al. Endotoxin-tolerant mice have mutations in Toll-like receptor 4 (Tlr4). *J. Exp. Med*. 1999;189:615–625.
 47. Conner JR, Smirnova II, Poltorak A. A mutation in Irak2c identifies IRAK-2 as a central component of the TLR regulatory network of wild-derived mice. *J Exp Med* 2009;206:1615–1631.
 48. Conner JR, Smirnova II, Poltorak A. Forward genetic analysis of Toll-like receptor responses in wild-derived mice reveals a novel antiinflammatory role for IRAK1BP1. *J Exp Med*. 2008; 205:305–314.
 49. Zhang J et al. Identification of new loci involved in the host susceptibility to *Salmonella* Typhimurium in collaborative cross mice. *BMC Genomics*. 2018;19:303.
 50. Montgomery TL et al. Interactions between host genetics and gut microbiota determine susceptibility to CNS autoimmunity. *Proc Natl Acad Sci USA*. 2020;117:27516–27527.
 51. Holt EA et al. Host genetic variation has a profound impact on immune responses mediating control of viral load in chronic gamma-herpesvirus infection. *J Immunol*. 2023;211:1526–1539.
 52. Carpenter S et al. A long noncoding RNA mediates both activation and repression of immune response genes. *Science*. 2013; 341:789–792.
 53. Robinson EK et al. lincRNA-Cox2 functions to regulate inflammation in alveolar macrophages during acute lung injury. *J Immunol*. 2022;202:1886–1900.
 54. Tyler AL et al. Epistatic networks jointly influence phenotypes related to metabolic disease and gene expression in diversity outbred mice. *Genetics*. 2017;206:621–639.
 55. Aydin S et al. Genetic dissection of the pluripotent proteome through multi-omics data integration. *Cell Genomics*. 2023; 3:100283.
 56. Saul MC, Philip VM, Reinholdt LG, Chesler EJ; Center for Systems Neurogenetics of Addiction. High-diversity mouse populations for complex traits. *Trends Genet TIG*. 2019;35:501–514.,
 57. Zhang MQ, Macala KF, Fox-Robichaud A, Mendelson AA, Lalu MM; Sepsis Canada National Preclinical Sepsis Platform. Sex- and gender-dependent differences in clinical and preclinical sepsis. *Shock*. 2021;56:178–187.

© The Author(s) 2025. Published by Oxford University Press on behalf of The American Association of Immunologists.

This is an Open Access article distributed under the terms of the Creative Commons Attribution-NonCommercial License (<https://creativecommons.org/licenses/by-nc/4.0/>), which permits non-commercial re-use, distribution, and reproduction in any medium, provided the original work is properly cited. For commercial re-use, please contact reprints@oup.com for reprints and translation rights for reprints. All other permissions can be obtained through our RightsLink service via the Permissions link on the article page on our site—for further information please contact journals.permissions@oup.com.

ImmunoHorizons, 2025, 9, 1–14

<https://doi.org/10.1093/immhor/vlaf007>

Research Article